Marked-up copy: in red the changes according to the requests of the Editor

in yellow the changes according to the requests of the Reviewer 1

in green the changes according to the requests of the Reviewer 3

Insights into 2- and 4(5)-Nitroimidazoles Decomposition into Relevant Ions and Molecules Induced by VUV Ionization

A. Cartoni,[1,2] A. R. Casavola,*[1] P. Bolognesi[1] M. C. Castrovilli,[1] D. Catone,[3] J. Chiarinelli,[1] R. Richter[4] and L. Avaldi[1]*

1) Istituto di Struttura della Materia (ISM), Consiglio Nazionale delle Ricerche (CNR) Area della Ricerca di Roma 1, via Salaria Km 29,300, Monterotondo Scalo (RM), 00016, Italy.

2) Dipartimento di Chimica, Sapienza Università di Roma, Pl.e Aldo Moro 5, 00185, Roma, Italy.

3) Istituto di Struttura della Materia (ISM), Consiglio Nazionale delle Ricerche (CNR), Area della Ricerca di Roma 2, via del Fosso del Cavaliere 10, 00133, Roma, Italy

4) Elettra Sincrotrone Trieste, Area Science Park, 34149, Basovizza, Trieste, Italy

ABSTRACT

Nitromidazoles are relevant compounds of multidisciplinary interest and the knowledge of their physical-chemical parameters as well as their decomposition under photon irradiation is needed. Here we report an experimental and theoretical study of the mechanisms of VUV photofragmentation of 2 and 4(5)-nitromidazoles, compounds used as radiosensitisers in conjunction with radiotherapy as well as high-energy density materials. Photoelectron–photoion coincidence experiments, measurements of the appearance energies of the most important ionic fragments, density functional theory and single-point coupled cluster calculations have been used to provide an overall insight into the energetics and the structure of the different ionic/neutral products of the fragmentation processes. The results show that these compounds can be an efficient source of relevant molecules CO, HCN, NO, NO_2 and produce ions of particular astrophysical interest, like the isomers of azirinyl cation (*m/z* 40), predicted to exist in the interstellar medium, and protonated hydrogen cyanide (*m/z* 28).

1.INTRODUCTION

It is well known that the specific role of a molecule is related to its physical-chemical properties and molecular structure.[1,2] The knowledge of these relationships in different fields of chemistry and physics is of fundamental significance and may help to design and synthesize new molecules relevant to medicine, material science and sensors.[3,4] Therefore, although not always straightforward, the establishing of these structure-properties correlations is of paramount importance. Recently in the study of 2- and 4(5)-nitroimidazoles radiosensitizer it has been proposed that possible radiosensitising mechanisms for these isomers depend on some of their characteristic fragmentation pathways. [5-7] The study of the major dissociation routes is of great interest also in other fields of chemistry, as for example in the identification of the most relevant ionic and neutral building blocks involved in the interstellar synthesis of nitrogen-containing molecules.[8] Furthermore, due to physical-chemical properties, such as the high heats of formation,[9] nitroimidazole derivatives are some of the most attractive nitrogen rich compounds used as high-energy density materials (HEDM).[10-12] Energetic materials store chemical energy and then, by decomposition, transform it into mechanical energy. Their fragmentation can be induced by different sources such as heat and sparks, which produce electronically excited molecules.[13,14] More energetic sources can also ionize these compounds leading to their dissociation into small ionic and neutral products, until now only partially identified and characterized, as in the case of 2- and 4(5)-nitroimidazoles.[15] Indeed, in addition to CO_2, N_2 and H_2O, other degradative toxic molecules or corrosive acids can be produced by combustion of a propellant, making that material an unsuitable green-friendly compound, for instance in defence and space applications.[16] Many efforts[17] are still devoted to identify the particles released in the environment after combustive and explosive processes and to evaluate their impact as contaminants. A complete overview of all possible decomposition products is therefore of fundamental and applicative interest. In the present work we performed a theoretical and experimental study of the mechanism of formation

of the most important ionic and neutrals species observed after irradiation of nitroimidazole isomers with VUV light. As for other ionized nitroaromatic compounds[18,19] and equally to the behaviour of nitroimidazoles after UV excitation,[14] the initial decomposition pathway is the release of nitro oxide molecule through a nitro-nitrite isomerization.**Errore. Il segnalibro non è definito.** In the past years many efforts have been devoted to analyze the mechanism of formation of NO but little or partial attention has been paid to the study of the mechanism of dissociation of the NO_2- group from the ring of 2- and 4(5)-nitromidazoles isomers .**Errore. Il segnalibro non è definito.**,[6] In a previous work**Errore. Il segnalibro non è definito.** it has been demonstrated that under VUV light absorption the breakup of the 4(5)-nitroimidazoles' ring, following the NO-loss (scheme 1), produces fundamental simple molecules: CO and HCN. The theoretical results show no evidence of the formation of N_2 molecules.

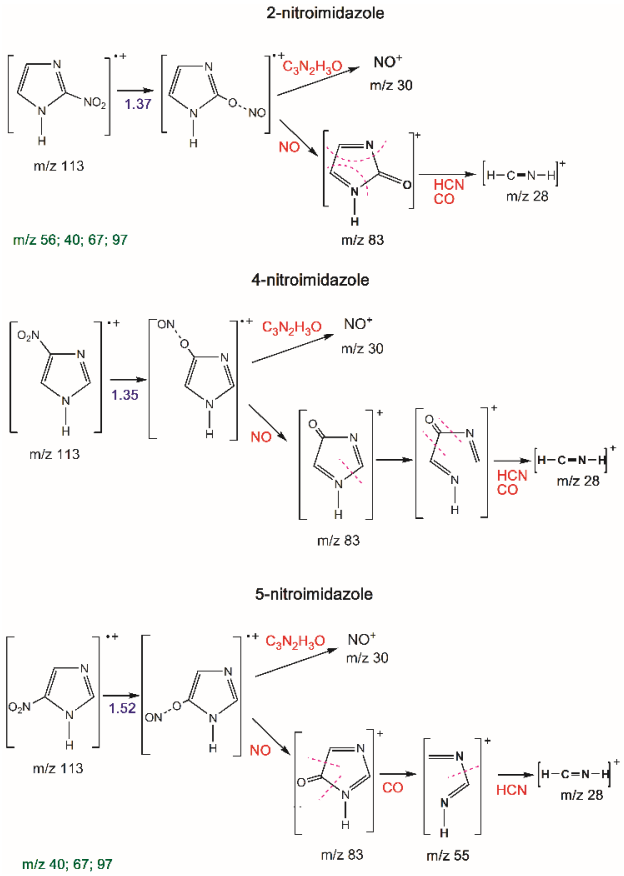

Scheme 1. Fragmentation pathways proposed for the three nitroimidazole isomers.[5] Numbers in blue (eV) are the energetic barriers relative to the parent ion (*m/z* 113). Text in red and green indicate, respectively, the neutrals released in the decompositions and the ions analyzed in this work. The most abundant ions observed are indicated in bold.

On the other hand, in 2-nitroimidazole an intense peak, corresponding to the undamaged ring (*m/z* 83) was observier. This work is focused on the investigation of the mechanism of formation of the other characteristic ions (*m/z* reported in green in scheme 1) not yet discussed. This is achieved by the experimental and theoretical determination of appearance energies (AEs) of the relevant fragment ions (scheme 1) observed in the mass spectra of 2- and 4(5)-nitroimidazoles and by Photoelectron–photoion coincidence (PEPICO) measurements.

2. Methods

The VUV induced photofragmentation of the nitroimidazole isomers has been studied with tunable synchrotron radiation at two different beamlines, at the Elettra storage ring in Trieste (Italy). The PEPICO experiments which allow to obtain ion-state selected mass spectra, have been performed at the Gas Phase beamline[20] while the AEs of the main fragment ions have been measured at the Cipo beamline.[21] As reported in literature[22,23] the 4-and 5- nitroimidazoles are almost degenerate in energy and in the gas phase coexist in a tautomeric equilibrium with a relative population of 1:0.7 (4-nitroimidazole:5-nitroimidazole) at 390 K. Hence in the following we will refer to 4(5)-nitroimidazoles, assuming that both isomers are present in the gas phase. The computational study of the three isomers at the B3LYP/6-311G++(d,p) level of theory with a single-point coupled cluster calculations, CCSD, of the energies has been crucial for the interpretation of the experimental results. For the sake of simplicity an ion will be indicated as *m/z* 83 or 83^+ and 2- and 4(5)-nitroimidazoles as 2-NIM and 4(5)-NIM, respectively.

2.1 Experimental details

The apparatus for the PEPICO experiments[24] and the related experimental procedures[25] for data acquisition and analysis have been described in details in previous publications.[26,27] Briefly, a VG 220i hemispherical electrostatic electron energy analyzer with multidetection capabilities and a time of flight (TOF) spectrometer are mounted opposite to each other at the magic angle with respect to the polarization direction of the linearly polarised incident radiation. The photoelectron and TOF

spectrometers can be operated independently, for the measurement of the photoelectron spectrum (PES) and of the mass spectrum, respectively, or in time coincidence for PEPICO experiments. The TOF analyzer is operated in pulsed extraction mode, triggered either by a pulse generator at 1 KHz, or by the detection of a kinetic energy resolved photoelectron. In the latter case (PEPICO mode), an additional trigger provided by a pulse generator at 100 Hz allows the measurement of the spectrum of random coincidences to be subtracted from the electron-ion coincidence measurements, following a proper normalization. The PEPICO measurements provide the state-selected photofragmentation spectra for fragmentation processes occurring on a time scale of less than 2μs. A fixed photon energy of 60 eV, an overall energy resolution of about 300 meV and a step size in kinetic energy of the order of 200-400 meV were used, resulting in a typical counting rate of less than 20 Hz of electrons and few tens of thousands of ions.

The AE measurements of ionic fragments produced from the photofragmentation of the molecular systems were performed in the photon energy range 5–17 eV by means of an Aluminum Normal Incidence Monochromator (Al-NIM). The experimental apparatus, described in detail elsewhere[28] consists of an ionization region where a set of ion optics extracts and focuses the ions produced by ionization via synchrotron radiation into a commercial quadrupole mass spectrometer equipped with a channeltron detector. The experiments consist in the acquisition of the mass spectra at a fixed photon energy (16 eV) and the measurement of the photoionization efficiency curves (PECs) of the selected fragment ions to determine their AEs. The PECs are obtained by reporting the yield of the fragment versus photon energy, scanning the undulator/monochromator in order to maintain the maximum flux at each given energy. The PECs were normalized to the photon intensity, which was measured simultaneously by a photodiode located at the end of the beamline. The photon energy was calibrated against the autoionization features observed in the Ar total photoionization efficiency spectra between the 3p spin orbit components. The contribution of the second order radiation in the photon energy range, 11-14 eV, was removed by comparing the measured Ar^+ ion yield to its ionization cross

section.[29] Below 11.7 eV a lithium fluoride filter was used to ensure the removal of higher order radiations.[28] The experimental AE values are determined by plotting on a linear scale the PECs and fitting straight lines to the background and to the ion signal in the threshold region. The photon energy at the intersection of these two lines is the experimental determination of the AE. For each fragment, the AE value reported in Tab. 1 was obtained by repeating the fitting procedure over an increasing range of data points until a stable and reproducible value was achieved. The different determinations were averaged and their dispersion provided the uncertainty, estimated to be of the order of 10-100 meV depending on the sharpness of the PEC onset. All samples, purchased from Sigma-Aldrich with purity higher than 98 %, are in the form of powders. They were placed in a crucible under UHV condition, and sublimated at a temperature of 337 K and 370 K for the 2- and 4(5)-nitroimidazoles, respectively.

2.2 Theoretical details

Quantum chemistry calculations have been performed at the level of Density Functional Theory (DFT). The geometries were optimized using the Becke, three-parameter, Lee-Yang-Parr (B3LYP) functional with the 6-311++G** basis set. The frequency analysis was based on the normal mode harmonic approximation.[30] All critical points were characterized as energy minima or transition state structures (TS) by calculating the harmonic vibrational frequencies at the same level of theory. They were also used to compute the zero-point and thermal energy corrections. The TS were unambiguously related to their interconnected energy minima by intrinsic reaction coordinates (IRC) calculations.[31,32] Accurate total energies were obtained by single-point for the B3LYP calculations. The outer valence vertical ionization energies (IE) were calculated using the outer valence Green function OVGF/6-311++G** methods.[33,34] All calculations were performed using Gaussian 09.[35] The calculated AE are at 298.15 K. For more details see also Tab. S1 and S2 in ESI. In all calculations the fragmentation has been considered to proceed from the ground state of the molecular ion.

Moreover the shape of the PES for singlet and triplet states has not been modelled because it is beyond the scope of the work.

3. RESULTS AND DISCUSSION

In Figures 1a and b the mass spectra of the isomers measured at the photon energy of 16 eV are shown.

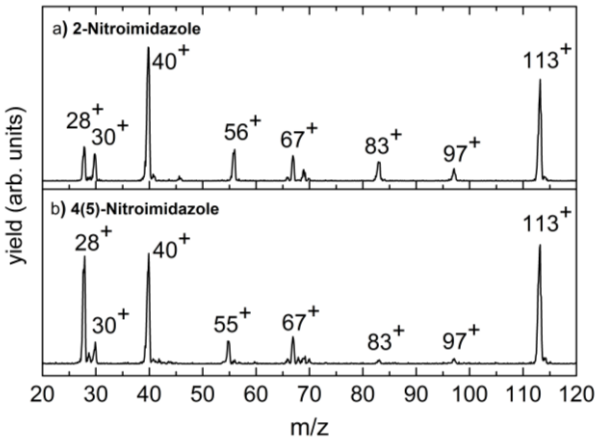

Figure 1. Mass spectra at the photon energy of 16 eV of a) 2-NIM and b) 4(5)-NIM acquired at the Cipo beamline.

The measured and calculated AE values are reported in Tab. 1 where the overall consistency between the measured AEs and the onset of the PEPICO signal (Figure 2) is evident. Due to the relatively large step size of the PEPICO measurements (of the order of a few hundreds of meV) the energy range, where the onset is located, is reported in Table 1. The structural details of the optimized geometries of the ions 40^+, 56^+, 67^+ and 97^+ analyzed in this work are shown in Figures S1 and S2 of ESI. The measured PECs are shown in Figures 3 and 6 and in Figures S3, S4 and S5 in the ESI. It is right to say that eventual fragment/neutral internal excitation and kinetic shift may contribute to the experimentally measured AEs, thus they have to be considered as an upper limit of the real AE values. Moreover the higher temperature of the experiment with respect to the room temperature used in the calculations does not appreciably affect the comparison.

Table 1. AE_{exp} and adiabatic AE_{th} (eV) of the fragments ions from 2 and 4(5)-NIM molecules. OVGF IE for Homo orbital is also reported in bold. Abbreviations: (s)=singlet; (d)=doublet; (t)=triplet.

NIM (113)	Ion/Neutrals	AE_{exp} PEPICO	AE_{exp}	IE_{th} and AE_{th}
2-NIM	113^+	9.4-9.6	9.54±0.01	9.35-**9.70**
	83^+/NO 30^+/$C_3N_2H_3O$	10.6-11.0 11.8-11.0	10.86±0.02 10.94±0.03	10.60
	56^+/NO+HCN 28^+/NO+HCN+CO	10.8-11.1 11.0-11.1	11.14±0.06 11.16±0.06	11.37
	97^+(d)/O (s)	13.9-14.1	13.9±0.2	13.89
	40^+(t)/NO_2+HCN 40^+(s)/NO_2+HCN	13.6-13.9	13.8±0.1	13.69 15.16
	67^+(t) /NO_2 67^+(s) /NO_2	12.75-13.62	12.76±0.06	11.64 12.09
4-NIM/5-NIM	113^+	9.5-9.6	9.59±0.010	9.50-**9.80**(5NIM) 9.40-**9.80**(4-NIM)
	83^+/NO 30^+/$C_3N_2H_3O$ 55^+/NO+CO 28^+/NO+HCN+CO	10.8-11.0	10.88±0.06 10.89±0.02 10.82±0.06 10.95±0.03	10.87(5-NIM) 10.60(4-NIM)
	97^+(d)/O(s)	13.8-14.2	14.18±0.02	13.81(5-NIM) 13.54(4-NIM)
	40^+(t)/NO_2+HCN	13.8-14.2	14.20±0.10	13.87(5-NIM) 16.00(4-NIM)
	40^+(s)/NO_2+HCN			14.28(5-NIM) 14.45(4-NIM)
	67^+(t)/NO_2	11.0-11.5	11.70±0.14	11.58(5-NIM) 11.46(4-NIM)
	67^+(s)/NO_2			12.43(5-NIM) 12.00(4-NIM)

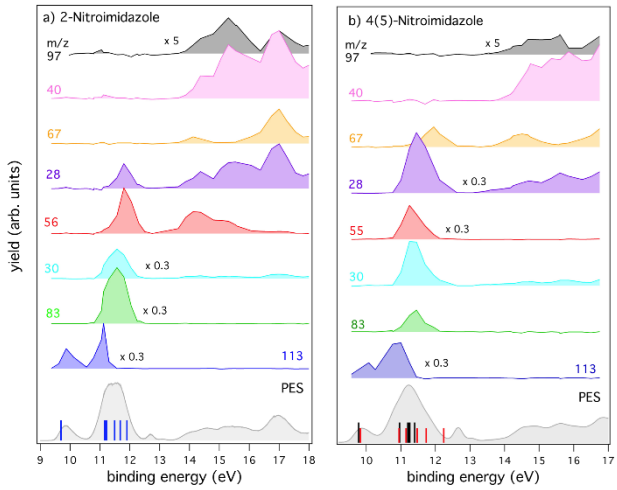

Figure 2. PEPICO spectra of the major fragments in the photofragmentation of 2-NIM (a) and 4(5)-NIM (b), see section 2.1. For each sample, the bottom panel reports the corresponding PES spectrum measured at 60 eV photon energy together with the theoretical position of the six lower molecular orbitals, labelled 29 to 24 for increasing binding energy, BE, calculated by the OVGF/6-311++G** method. In the b) panel, the black and red (i.e. longer and shorter) bars represent the contribution of the 4- and 5-NIM, respectively. The energy position and the Hartree Fock charge distribution of these

molecular orbitals are reported in Table S3 and Figure S6 of the ESI. Features at 12.6-13.0 eV are due to some water contamination.

3.1 2-nitroimidazole

The PECs for fragments 30^+ and 83^+, 28^+ and 56^+ are shown in Figure 3.

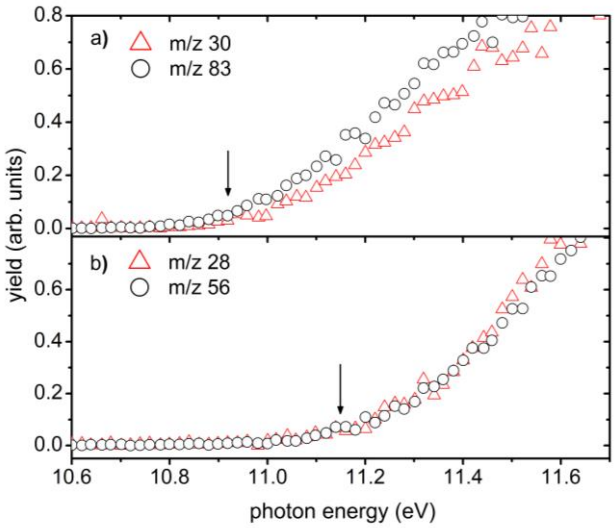

Figure 3. PECs of the 2-NIM fragment ions at a) *m/z* 83 and 30 and b) *m/z* 56 and 28. The threshold region is indicated by the arrow.

The theoretical adiabatic ionization energy (IE) 9.35 eV of the 2-NIM is in agreement with the experimentally determined IE (see ESI Figure S4a) of 9.54±0.01 eV while the OVGF value, 9.7 eV, is higher since it represents the vertical ionization energy. The measured AEs of ions at *m/z* 83 and 30 are very similar (Figure 3a), being 10.86±0.02 and 10.94±0.03 eV, respectively (Table 1). These data are in agreement with the fragmentation pathway, proposed in the previous work[5], where the two ions are formed via the same TS with an energy barrier of 1.37 eV (scheme 1). This results in an adiabatic AE of 10.60 eV.[36] The identification of the routes leading to the two fregment ions 40^+ and 56^+, the latter being also source of the ion 28^+ as shown below, has been very challenging. As for the ion at *m/z* 56, the HCN-loss route has been considered (Figure 4).

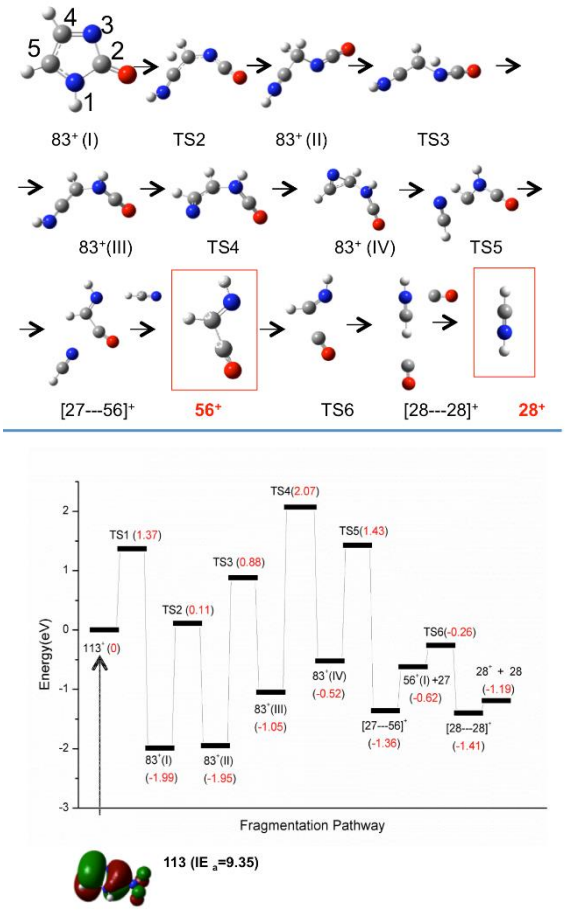

Figure 4. Fragmentation pathway of 2-NIM parent ion (113^+, I) leading to 56^+ and 28^+ fragments. Top: the optimized geometries of the species from isomer 83^+(I) at the B3LYP/6-311++G** level of theory. Bottom: The total relative energy (in eV with zero point energy, ZPE) at the CCSD/6-311++G** level of theory with respect to the parent ion, and the HOMO orbital of 2-NIM molecule.

The pathway starts, after the NO-release, with the breaking of the N1-C2 bond in the 83^+ (I) ring isomer (-1.99 eV) and the H migration from C5 to C4, which produces the 83^+ (II) open chain isomer (-1.95 eV) through an energy barrier of 2.10 eV (TS2, 0.11 eV). Afterwards, two other 83^+ isomers are formed: 83^+(III) (-1.05 eV) with the migration of the H in C4 to N3 via TS3 (0.88 eV), and 83^+ (IV) (-0.52 eV) where a three element ring, HCNCH, is formed after the H migration from N1 to C5 via TS4 (2.07 eV). From the 83^+ (IV) the hydrogen cyanide molecule, HCN, and the 56^+ ion (-0.62 eV) with HNC(H)CO connectivity are produced through TS5 (1.43 eV). The species 56^+ can further

dissociate through TS6 (-0.26 eV) in CO and $[HCNH]^+$ ion (*m/z* 28). In this pathway the TS at the highest energy, TS4, leads to an adiabatic AE for both 56^+ and 28^+ of 11.37 eV, in reasonable agreement with the measured AEs 11.14±0.06 eV and 11.16 ± 0.06 eV for 56^+ and 28^+, respectively (Table 1, Figure 3b). This clearly proves that 28^+ is the daughter ion of 56^+. The study of the *m/z* 40 ion has been intriguing since this ionic fragment appears at higher energy than the other ions, as shown by the measured value of the AE (40^+) = 13.8±0.1 eV (Table 1, Figure S4c in ESI) which suggests a different decay route. Since the ion 40^+ is also observed in the mass spectrum of imidazole[18,37,38] the fragmentation pathway from 67^+ $[113\text{-}NO_2]^+$ has been considered. Other routes, starting for instance from the C-C or N-C breaking and before NO_2-loss or associated with H transfer to C2[37,38] are not analyzed here. Both the fragmentations from 67^+ ions in the singlet and triplet states have been considered, as shown in Figure 5. The ring ion 67^+ (I,t) in triplet state is more stable than the singlet one by 0.63 eV (see Table S1) and leads to the 40^+ ion through the energy path (a) in Figure 5.

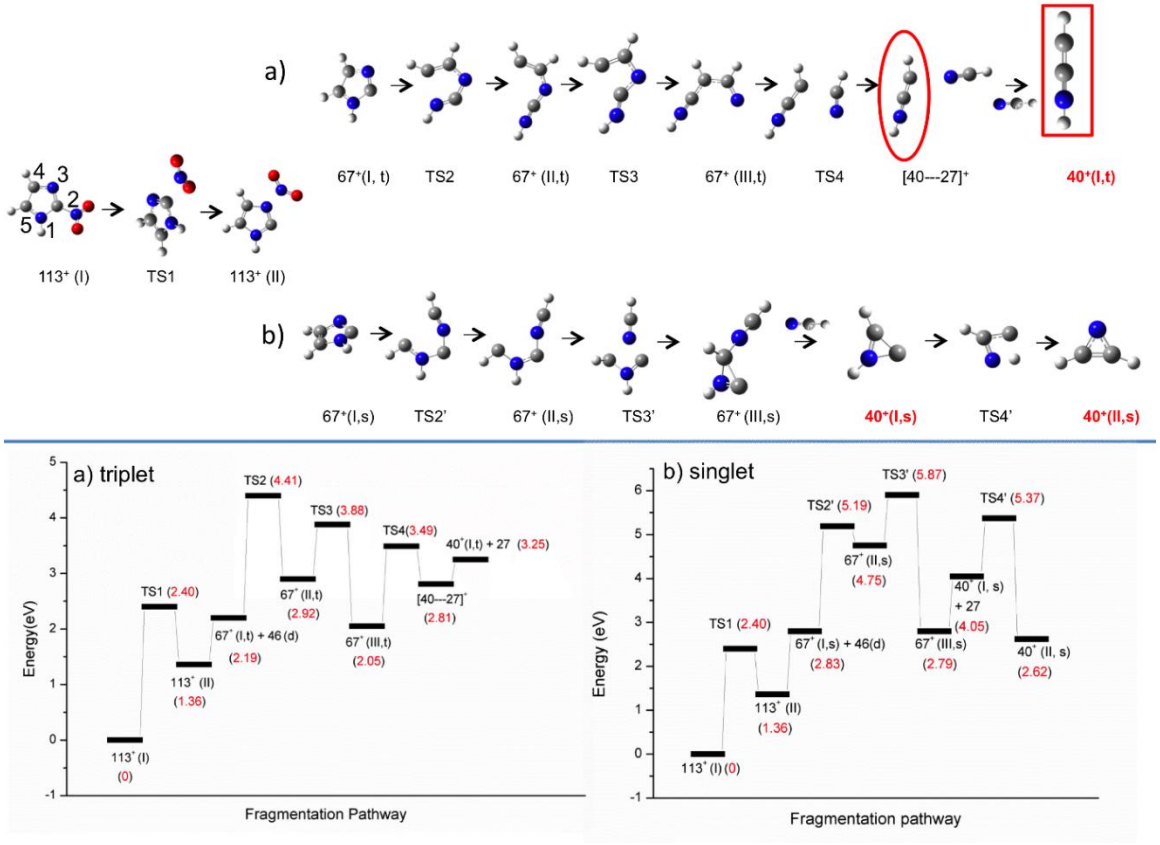

Figure 5. Fragmentation pathways a) and b) of 2-NIM parent ion (113^+,I) leading to 40^+ in triplet and singlet states. Top: the optimized geometries of the species from parent ions at the B3LYP/6-311++G** level of theory. Bottom: the total relative energies (in eV with zero-point energy, ZPE) at the CCSD/6-311++G** level of theory with respect to the parent ion.

The fragmentation starts from the parent ion 113^+ (I) which isomerizes into the 113^+ (II) via TS1 (2.40 eV) and produces the NO_2 molecule and the 67^+ ions, in triplet (a) or singlet (b) state. In the triplet state, the ring opens with the breaking of N1-C5 bond and the isomer 67^+(II,t) is formed at 2.92 eV through TS2 (4.41 eV). Then, via TS3 (3.88 eV) the H-N1-C2 moiety shifts on C5 and a new bond is formed between C2-C5 producing the 67^+(III,t) isomer (2.05 eV) with HNC2C5(H)C4(H)N connectivity. Further, the C4-C5 bond breaks through TS4 (3.49 eV) producing an ionic adduct (2.81 eV) between the quasi-linear triplet ion 40^+ HNCCH and HCN. Finally, the ion 40^+(I,t) is formed. Considering the TS at higher energy (TS2), this route leads to an adiabatic AE (40^+,t) of 13.69 eV in complete agreement with the experimental AE of 13.8±0.1 eV and consistent with the energy range 13.6-13.9 eV obtained in the PEPICO measurements (Figure 2a).

In the singlet 67^+(I,s) ion, the ring is initially broken at the C4-C5 bond via TS2' (5.19 eV) generating the 67^+(II,s) isomer (4.75 eV). Through the N3C4H shift via TS3' (5.87 eV) the 67^+ (III,s) isomer is formed (2.79 eV) with new bonds between N3-C5 and C2-C5 resulting in a three element ring. This isomer is the precursor of HCN and the cation 40^+(I,s) (4.05 eV) which in turn can isomerize, through the TS4' (5.37 eV) into the more stable ring isomer azirinyl ion 40^+(II,s), (2.62 eV), where both hydrogen atoms are bound to the carbon atoms (HCNCH).[39] However this path b) give a calculated AE (40^+, s) via the TS3', 15.16 eV, too high relative to the experimental AE (40^+) of 13.8±0.1 eV .

The formation of the ion 67^+ in the triplet and singlet states from routes a) and b) respectively, is not completely well understood. The calculated AE (67^+) of 11.64 (t) and 12.09 (s) eV, do match neither the measured AE nor the PEPICO measurements, which report values around 12.8 eV. A tentative explanation of this difference might be that other unexplored routes to 67^+, like the breaking of the ring 113^+ (I) before the NO_2-loss, are effective at higher energy. From Table S2 in ESI, it is also possible to evaluate the AE (67^+) in triplet and singlet states considering the neutrals NO(doublet), O(singlet) and O(triplet). However the obtained data do not match the experimental results, which set

the threshold value at 12.76 eV. Indeed for the less energetic path: 67^+(t) + NO(d) and O(t), the AE has been calculated to be 13.72 eV. In conclusion the interpretation of the AE for the 67^+ in 2-NIM remains an open question. Also, it should not be forgotten that all calculations are performed in the ground electronic state. This provides a good description for most cases, but might fail when the peculiarities of an excited electronic state drive alternative fragmentation paths.

The formation of the ion at *m/z* 97 has been also considered (see Fig S4b in ESI). It is produced through the atomic oxygen-loss from 113^+ parent ions. The experimental AE (97^+) is 13.9±0.2 eV in agreement with the PEPICO results: 13.9-14.1 eV (Table 1 and Fig 2a). Considering the oxygen atom and 97^+ in the triplet and doublet states respectively, an AE (97^+) of 11.39 eV was derived by theoretical calculations. On the other hand considering the oxygen atom in the singlet state an AE of 13.9 eV was calculated (see Table S2), which is consistent with the experimental observation. The same conclusions were obtained with the calculations performed at MP2 level of theory (data not shown). It is worth saying that a high spin contamination was revealed for this radical cation 97 as indicated by the ⟨S2⟩ operator, far from the theoretical value for the pure doublet spin state (0.75). We also consider the ion 97^+ in quadruplet state. In such a case there is small spin contamination, but the theoretical data (12.81 eV, Table S2 in ESI) do not match the experimental results. The presence of a barrier or the contribution of specific excited electronic states to 97^+ cannot be excluded.

3.2 4(5)-nitroimidazoles

The theoretical adiabatic ionization energy (IE) of 9.40 and 9.50 eV for the 4- and 5-NIM, respectively, is in agreement with the experimentally determined IE (see ESI Figure S3 and S5a) of 9.59±0.01 eV while the OVGF value is 9.8 eV (Tables 1 and S3). As also reported in previous work[Errore. Il segnalibro non è definito.] the ions 83^+, 55^+, 30^+ and 28^+ should appear at the same energy through the TS at 1.35 eV (4-NIM) and 1.52 eV (5-NIM) (scheme 1). Indeed the calculated AE values are

10.60 and 10.87 eV for 4- and 5-NIM respectively, in agreement with the measured ones: 10.88 ± 0.06 (83^+), 10.89 ± 0.02 (30^+), 10.82 ± 0.06 (55^+) and 10.95 ± 0.03 (28^+) eV (Figure 6 and Table 1).

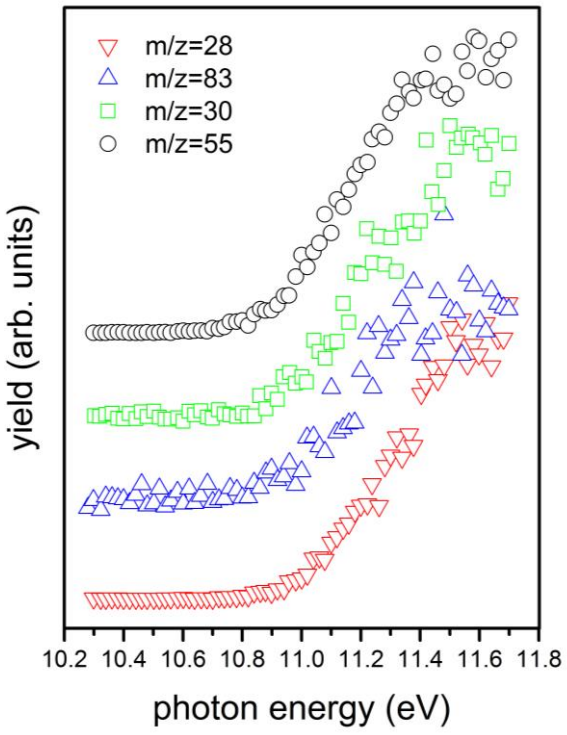

Figure 6. PECs of the 4(5)-NIM fragment ions at *m/z* 28 in red, 83 in blue 30 in green and 55 in black.

The PEPICO results confirm these data (Figure 2b, Table 1). As for the fragment ion at *m/z* 40 its measured AE is 14.2 ± 0.1 eV (Figure S5c in ESI) and matches quite well the PEPICO experiments where an AE range of 13.8-14.2 eV has been evaluated (Table 1 and Figure 2b). Theoretical calculations have been also performed considering the formation of the ions at *m/z* 67 (I) in its singlet and triplet states after the loss of NO_2 for both 4 and 5-NIM. In the case of 5-NIM the triplet state of 67^+ is more stable than the singlet one by 0.83 eV (see Table S1). The two fragmentation pathways a) and b) leading to 40^+ and the molecular structures and energetics of the minima and transition states for 5-NIM are reported in Figure 7. As in the case of 2-NIM, the triplet and singlet states of the 67^+ ions lead to the open chain and cyclic cation $C_2H_2N^+$ respectively.

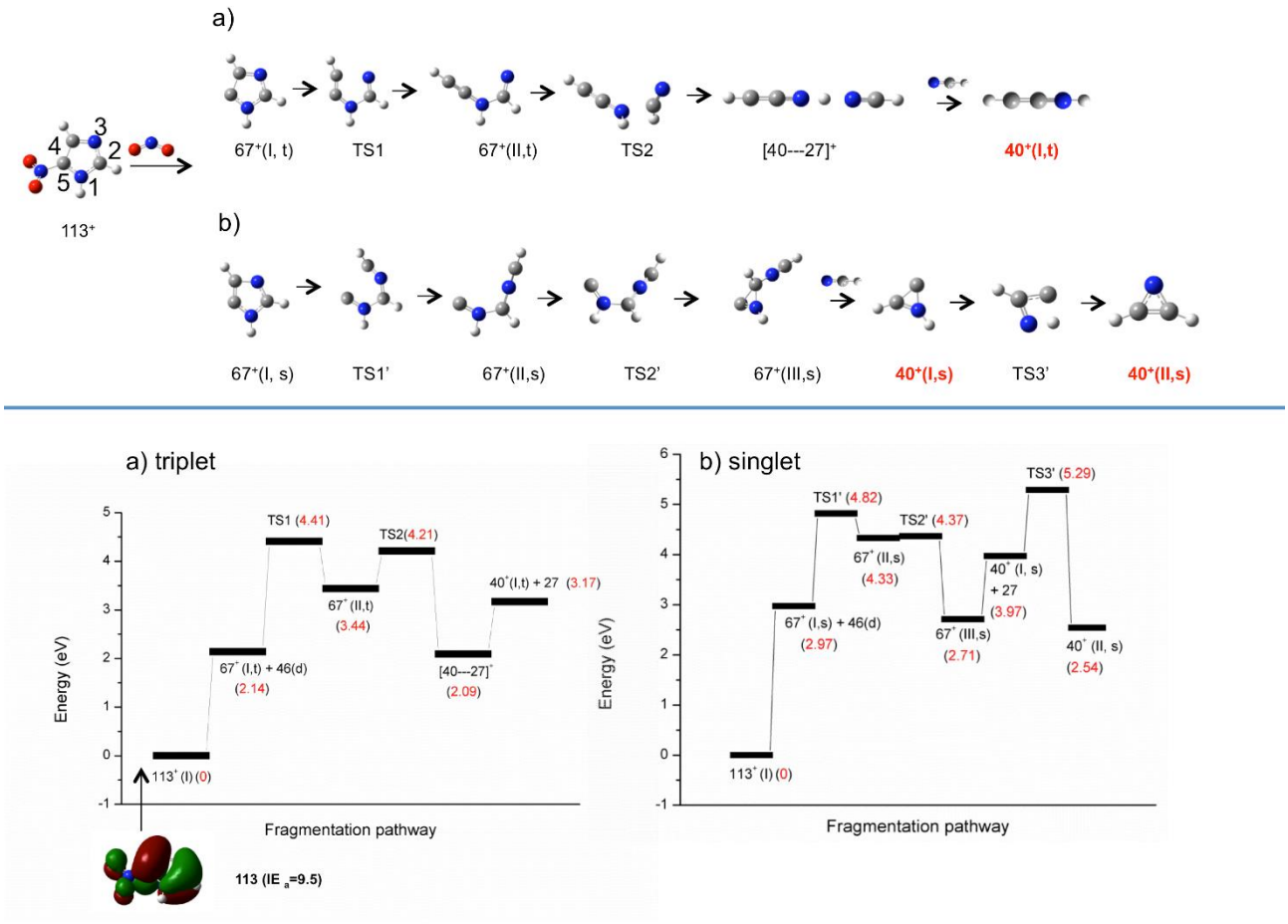

Figure 7. Fragmentation pathways a) and b) of 5-NIM parent ion (113^+,I) leading to 40^+ triplet and singlet. Top: the optimized geometries of the species from parent ions at the B3LYP/6-311++G** level of theory. Bottom: the total relative energy (in eV with zero point energy, ZPE) at the CCSD/6-311++G** level of theory with respect to the parent ion and the HOMO orbital of 5-NIM molecule.

The pathway a) starts with the breaking of N3-C4 bond in the ring of the 67^+(I,t) ions (2.14 eV) and leads, through TS1 (4.41 eV), to the 67^+(II,t) isomer (3.44 eV) where the already preformed quasi-linear $HCCNH^+$ (40^+) and HCN molecule are present. Hence, via TS2 (4.21 eV) the $[40---27]^+$ (2.09 eV) complex is formed and this eventually produces the 40^+ (I, t) and HCN (3.17 eV). According to this pathway the calculated adiabatic AE of 40^+ (I, t), based on TS1 energy, is 13.87 eV to be compared with the measured AE 14.2 ± 0.1 eV (Table 1). The route b) from the singlet state of the ring 67^+(I,s) isomer (2.97 eV) begins with the fission of the C4-C5 bond via TS1' (4.82 eV) leading to the open chain isomer 67^+(II,s) (4.33 eV) that with a very low barrier of 0.05 eV via TS2' (4.37 eV) forms the 67^+(III,s) isomer (2.71 eV) where the preformed cyclic cation isomer is present and it

is produced after the detachment of HCN (3.97 eV). Then through TS3' (5.29 eV) the 40^+(I,s) can evolve in the more stable isomer 40^+(II,s) (2.54 eV). Considering this route and the TS1' energy the calculated AE of 40^+(I,s) is 14.28 eV in agreement with both PEPICO results and the measured AE (Table 1). To calculate the AE of 40^+(II,s) the TS3' must be considered and an AE=14.80 eV is obtained. From the analysis of these data one may conclude that both pathways a) and b) are operative. If the AEs of the 67^+ ions in the triplet and singlet states are also considered according to these routes, the calculated AEs of 67^+ are 11.58 and 12.43 eV, respectively. It is evident from Table 1 that only the first one is in agreement with the experimental data (measured AE of 67^+ is 11.70±0.14 eV and the PEPICO energy range is 11.0-11.5 eV). As for the ion at *m/z* 97, the same theoretical considerations discussed for 2-NIM are valid. The experimental AE (97^+) value is 14.18 ± 0.02 eV in agreement with the energy range of PEPICO data (Figure 2b), while the calculated 13.81 (5-NIM) and 13.54 eV (4-NIM) are obtained considering the 97^+ and oxygen atom in the doublet and singlet states, respectively (see Table 1 and Table S2 in ESI). Considering the ion 67^+ in triplet and singlet states from 4-NIM, the experimental AE=11.70±0.14 eV and the theoretical AEs: AE(67^+,s)=12.00 eV and AE(67^+,t)=11.46 eV, show that probably 67^+ ion in both singlet and triplet states may be formed (Table 1 and Figure 8) even if the lower theoretical value is more reliable. As for ion 40^+ the calculated fragmentation pathways from 4-NIM lead to isomers higher in energy than the 40^+ isomers in singlet and triplet states obtained for the 2 and 5-NIM compounds (Table S1 and Figure 8 top). In pathway a) the breaking of the N1-C2 bond via TS1 (3.76 eV) leads to 67^+(II,t) isomer (3.30 eV) that in turn, after the fission of the N3-C4 bond through TS2 (6.00 eV) and the formation of $[40\text{---}27]^+$ complex (5.37 eV), produces the high energy 40^+ (II,t) ion (6.63 eV) in the triplet state with HNC(H)C connectivity. In pathway b) there is always the breaking of the N1-C2 bond via TS1'(4.30 eV), but 67^+(II,s) (3.80 eV) isomerizes into 67^+(III,s) (0.89 eV) after the migration of H from C5 to C4 via TS2' (4.22 eV). Then the fission of the C4-C5 bond produces, via TS3' (4.40 eV) and $[40\text{---}27]'^+$ complex (4.17 eV), the HNC and the high energy open chain 40^+ (III,s) with HCNCH connectivity. The evaluated theoretical AEs (40^+) are 16.0 and 14.45 eV for triplet and singlet respectively, the

latter being comparable with the experimental value of 14.20 ± 0.10 eV. Considering these results it is possible to conclude that the 5-NIM and 4-NIM isomers can contribute to ion 40^+ in the low energy triplet and high energy singlet states, respectively. However other dissociation routes, not explored or found in this work, cannot be excluded.

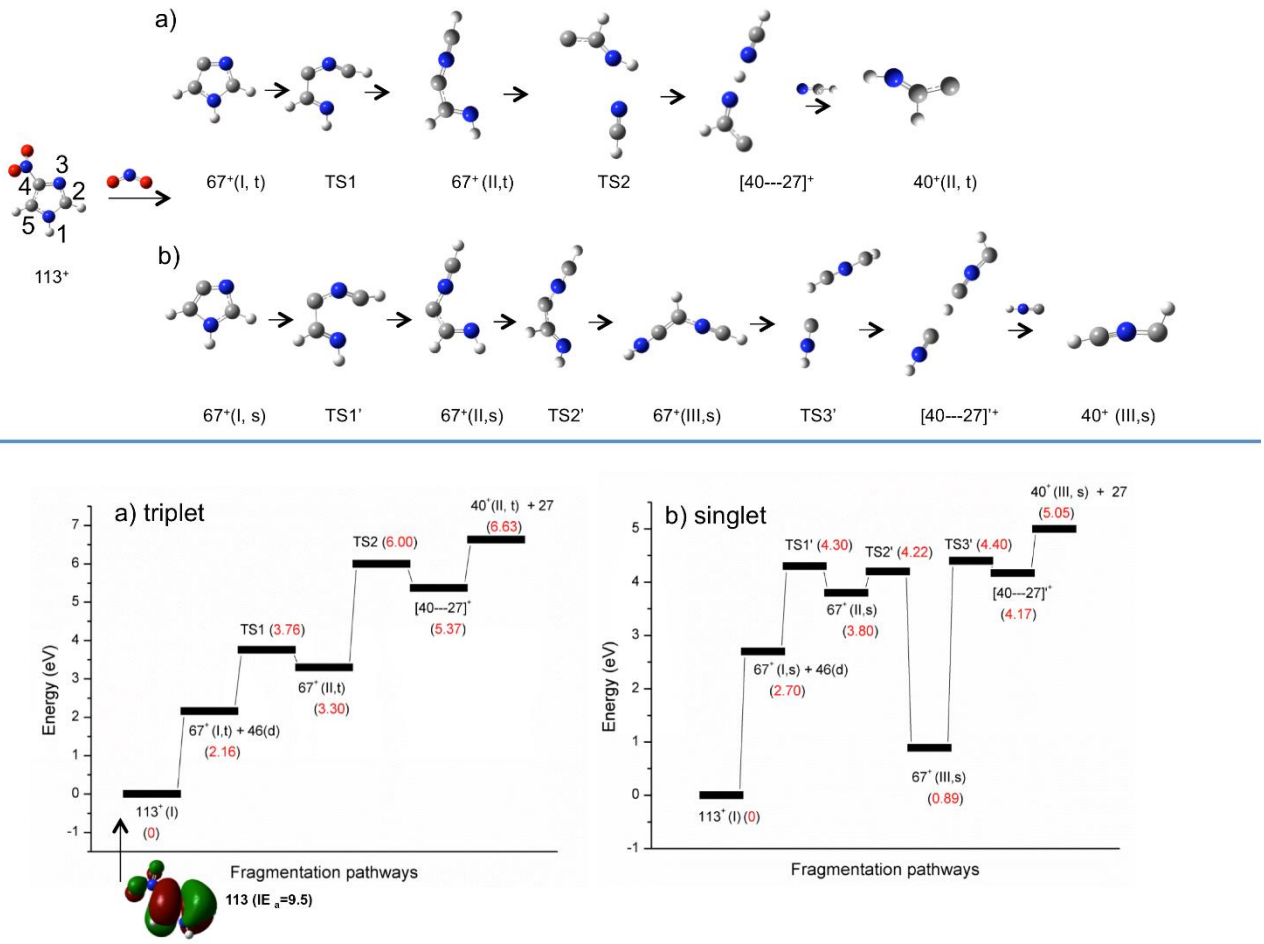

Figure 8. Fragmentation pathways a) and b) of 4-NIM parent ion (113^+, I) leading to 40^+ triplet and singlet states. Top: the optimized geometries of the species from parent ions at the B3LYP/6-311++G** level of theory. Bottom: the total relative energy (in eV with zero-point energy, ZPE) at the CCSD/6-311++G** level of theory with respect to the parent ion and the HOMO orbital of 4-NIM molecule.

3.3 PEPICO measurements

The PES spectra of nitroimdazole isomers reported in the bottom panels of Figures 2 display the HOMO (orbital 29 in Table S3 and Figure S6 in ESI) just below 10 eV well separated by the other

features, a broad band which involves orbitals 28-24 centered at 11.5 eV and then the manifold of features which correspond to inner valence orbitals. The PES spectrum of the 4- and 5-NIM has been reported in a previous paper. [23] A good agreement between the two measured spectra exists. In ref [21] the binding energies of the different orbitals have been calculated with the OVGF/6-311+G** and SAOP/et-pVQZ models. The OVGF predictions well match the experimental spectrum as the present OVGF calculations performed with 6-311++G** basis set (Figure 2 and Table S3). As already observed in the case of pyrimidine[24] and halogenated pyrimidines,[25] the PEPICO spectra of nitroimidazoles (Figures 2) display a correlation between molecular orbitals (MO) and peculiar fragmentation patterns. In ref. [23] this state-selective fragmentation, which is ruled by the channel with the nearest AE, has been qualitatively rationalised in terms of the charge distribution of the different MOs. In the nitroimidazoles, the parent ion is observed exclusively in the lower ionic states, i.e. below the lowest AE at about 11 eV. This demonstrates that as soon as a fragmentation channel is opened, in the present case the loss of the NO as neutral or charged species, the molecule will certainly fragment, at least within the μs time scale of our experiment. The formation of the fragments 83^+ and 30^+ are the first energetically allowed channels and correlate to the same MOs, in the second band at binding energy 11-12 eV (Figure 2). The fragment 83^+ in all isomers is an example of a state-selective fragmentation. In fact, its source can be unambiguously tracked down to the MOs 28-24 around 11-12 eV (Table S3). Another example of stringent state-selective fragmentation is provided by fragment 55^+ in 4(5)-NIM, again correlated to the MOs at 11-12 eV. Even thought to a minor extent, fragment 30^+ presents a similar picture, apart for a weak but not negligible signal in the inner valence region. Fragment ions 55^+ and 56^+ are present exclusively in 4(5)- and 2-NIM, respectively, at least in the binding energy region explored in this work. In this respect, they can be considered as 'fingerprints' of their source molecules. At variance, while 55^+ can be uniquely related to the MOs at 11-12 eV, the fragment 56^+ in 2-NIM does not show any marked state selectivity, and its origin can be related to MOs at 11 eV < BE < 16 eV. This confirms, as already discussed in the previous section and in ref [**Errore. Il segnalibro non è definito.**], that they originate by different fragmentation

pathways in the different isomers, where ring opening and fragmentation of 83^+ produce $[HNC(H)NCH]^+$ + CO for 55^+ in 5-NIM and $[HNC(H)CO]^+$ + HCN for 56^+ in 2-NIM. Fragment 28^+ is observed in all isomers with a similar behaviour and an overall lack of state-selectivity. Consistently with the AE measurements reported in Table 1, the PEPICO spectra show that the group of fragments 83^+, 30^+, $56^+/55^+$ and 28^+ have a common route of formation in their threshold region, with the clear involvement of MOs in the BE region 11-12 eV. This supports the explanation provided in the previous section of successive processes, all originating with the NO-loss from the parent ion. However, in the 2-NIM PEPICO spectrum the most intense features are due to fragments 83^+ and 30^+, while the fragments 28^+ and 55^+ provide the major contribution to 4(5)-NIM PEPICO spectrum as already rationalized and discussed in previous work.**Errore. Il segnalibro non è definito.** For all of these fragments the MOs at BE 11-12 eV seem to play a crucial role, in terms of state-selective fragmentation (fragments 83^+ and 55^+) as well as for its peculiar behaviour in the different isomers (stability of fragment 83^+). Fragment 67^+, due to the loss of the entire NO_2 group, is probably the most intriguing feature in the photofragmentation spectrum of the NIM isomers. As already observed in Table 1, its AEs differ in the nitroimidazole isomers by more than 1 eV. Figure 2 clearly shows that its formation via the second band is only possible in the 4(5)-NIM, which is the reason of the energetic shift. However, this different behaviour in the formation of 67^+ could not be explained in the calculations of the fragmentation dynamics. Looking in a qualitative way at the charge distributions of MOs 28 and 27 (Figure 6S in ESI) one may observe that in 4-NIM these are bonding orbitals between the NO_2 group and the imidazole ring, while this is not the case in the 2-NIM. Finally, fragments 40^+ and 97^+ correlate to MOs towards the inner valence region, consistently with their larger AE values, showing small differences in their distribution of intensities, and no state-selectivity.

4. CONCLUSIONS

The role of nitroimidazole isomers as a source of relevant ions and neutrals after the interaction with the VUV light has been highlighted by the combination of AE measurements, PEPICO experiments, DFT and CCSD calculations of the fragmentation dynamics. NO_2, NO, CO and HCN molecules are stable neutrals released by all isomers and their production represents the main focus of the fragmentation pathways explored in this work. As for the ionic counterparts we have observed:

- Ion 28^+ $[HCNH]^+$: the linear isomer in the singlet state[40] is the lowest energy structure and it is formed in the fragmentation of all nitroimidazole isomers,[41-43] making reasonable to think that this ion might take part in the interstellar synthesis of heterocycle compounds.[44,45] Actually the $[HCNH]^+$ is an important species in the interstellar environment detected for the first time in 1986[46] and demonstrated to be abundant in the Titan's atmosphere by Cassini Huygens mission and a possible building block of more complex molecules.[47]

- Ion 56^+ $[HNC(H)CO]^+$: it is observed only in the mass spectrum of 2-NIM. It is formed through the HCN-loss from the imidazole ring and it is the precursor of $HCNH^+$ ion and CO molecule.

- Ion 55^+ $[HNC(H)NCH]^+$: it is present only in the mass spectrum of 4(5)-NIM isomers and it is a precursor of $HCNH^+$ and HCN species.

- Ion 67^+ imidazole ring $[C_3H_3N_2]^+$: both the triplet and singlet state of 67^+ have been considered. The triplet state is more stable than the singlet and no energy barrier was found for its formation from 113^+ (nitroimidazole) in 4(5)-NIM. In the case of 4(5)-NIM the theoretical AEs of 67^+(I, t) are in agreement with the experimental result while the calculated AE of 2-NIM is lower than the experimental value.

    - Ion 40^+ $[C_2H_2N]^+$: its formation from the imidazole ring at *m/z* 67^+ has been studied, taking into account both the triplet and singlet state of 67^+. In both states the calculated structures for 40^+ reflect the more stable ones recently re-discussed.[39] The singlet cyclic isomer azirinyl cation with C(H)NC(H) connectivity, the lowest structure in energy, is predicted from the

fragmentation of 2 and 5-NIM after the isomerization of the cyclic isomer C(H)N(H)C ion. Their calculated energy difference of 1.42 eV is in good agreement with the value of 1.49 eV found for these isomers by W-K Li *et al.*[48] Moreover the 4-NIM also produces a high energy isomer 40^+ with C(H)NC(H) connectivity that has been also found by Maclagan et al in the study of $C_2H_2N^+$ isomers.[49] As for the analysis of the potential energy surface of the triplet state, the ion 40^+ of the lowest energy is linear with HCCNH connectivity and it is 0.62 eV (Table S1) above the energy of singlet cyclic azirinyl cation 40^+ in agreement with the data of 0.63 eV (48.5 + 12.7 kJ mol^{-1}) reported by M. Frankowski *et al.*[50] It is noteworthy (Figure 5) that the linear triplet ion 40^+(I) is a quasi-linear ion in the $[40\text{---}27]^+$ complex before the dissociation and when the minimum geometry is calculated at the MP2 level of theory (Figure S1), in agreement with T. J. Lee and W-K Li *et al.*[39,48] Moreover the high energy open chain ion 40^+ in the triplet state with HNC(H)C connectivity (Figure 8 and Figure S1) formed by 4-NIM ion is another possible isomer and to the best of our knowledge it has not been analyzed in previous works probably because of its too high energy.

The difference between the calculated and measured AE of ion 67^+ in 2-NIM is puzzling. Considering our experimental approach and the theoretical description, several possible explanations have been considered. The first one is the existence of metastable states. From the experimental point of view, the TOF measurements of the PEPICO spectra and the QMS measurements of the AE values do involve quite different detection times, varying from few to several microseconds, respectively. Nevertheless, they provide consistent results, as shown in Table 1 suggesting that metastable states in this time scale, if present at all, do not play a major role. On the other hand, 'faster' processes, occurring on a time scale shorter than the extraction time (500 ns) of our set up**Errore. Il segnalibro non è definito.** are not 'seen' and the detected daughter ion will be considered as the result of a prompt fragmentation. This is a quite general situation in mass spectrometry, where "observed processes" depend on the time detection limit of the used spectrometers. Therefore, it is in principle possible that

a ‘fast’ process in 2-NIM, for example a curve crossing, is responsible for the instability and fast fragmentation of the 67^+ ionic ring. A second consideration is related to the calculations which consider as a starting point of the dynamics the ground state of the molecular ion, neglecting any involvement of excited ionic states. This approach is based on the observation that ultrafast decays to the ground ionic state via conical intersections are likely processes.[51-53] It is however possible that such description does not always apply, and that a ground state calculation does not provide a faithful or comprehensive description of the process. Furthermore it is possible that an energy barrier or a yet unidentified route that rapidly fragments 67^+ into a smaller daughter ion. In conclusion the formation and the structural and energetic characterization of the main neutrals and ions from VUV physical-chemical properties have been measured and calculated. This study can provide relevant insight into the chemical reactions of formation of the five-membered heterocycles containing nitrogen in the space and highlight the role of important astrophysical ions as $HCNH^+$ and $C_2H_2N^+$ isomers.

AUTHOR INFORMATION

Corresponding Authors

* A. Cartoni. E-mail: antonella.cartoni@uniroma1.it; Tel. + 39 06 49913678

* A. R. Casavola. E-mail: annarita.casavola@cnr.it; Tel. + 39 06 90672222; Fax +39 06 90672238

Notes

The authors declare no competing financial interests.

ACKNOWLEDGEMENTS

Work partially supported by the Italian Ministry of Foreign Affairs via the Serbia–Italy Joint Research Project (MAECI): “A nanoscopic view of radiation-biomatter interaction” PRG 220. A.C. thanks Prof. Stefano Borocci for the helpful discussions.

SUPPORTING INFORMATION. More details on theoretical calculations and experimental measurements are supplied as Supporting Information

REFERENCES

(1) Balzani, V.; De Cola, L. *Supramolecular Chemistry* Book NATO ASI Series **1992**,*371*. Springer Netherlands.

(2) Hover, R. Composition, Molecular Structure, and Physicochemical Properties of Tuber and Root Starches: a Review *Carbohydrate polymers* **2001**, *45*, 253-267.

(3) Cartoni, A.; Bolognesi, P.; Fainelli, E.; Avaldi, L. Photofragmentation Spectra of Halogenated Methanes in The VUV Photon Energy Range *J. Chem. Phys.* **2014**, *140*, 184307 (pp 13).

(4) Venditti, I.; Cartoni, A.; Fontana, L.; Testa, G.; Scaramuzzo, F. A.; Faccini, R.; Terracciano, C. M.; Camillocci, E.S.; Morganti, S.; Giordano, A. *et al.* Y^{3+} Embedded in Polymeric Nanoparticles: Morphology, Dimension and Stability of Composite Colloidal System *Colloids and Surfaces A: Physicochemical and Engineering Aspects* **2017**, *532*, 125-131.

(5) Bolognesi, P.; Casavola, A. R.; Cartoni, A.; Richter, R.; Markus, P.; Borocci, S.; Chiarinelli, J.; Tošić, S.; Sa'adeh, H.; Masič, M. et al, Communication: "Position" Does Matter: The Photofragmentation of The Nitroimidazole Isomers *J. Chem. Phys.* **2016**, *145*, 191102 (pp 5).

(6) Feketeova´, L.; Postler, J.; Zavras, A.; Scheier, P.; Denifl, S.; O'Hair, R. A. J. Decomposition of Nitroimidazole Ions: Experiment and Theory *Phys. Chem. Chem. Phys.*, **2015**, *17*, 12598-12607.

(7) Ribar, A.; Fink, K.; Probst, M.; Huber, E. S.; Feketeová, L.; Denifl, S. Isomer Selectivity in Low-Energy Electron Attachment to Nitroimidazoles *Chem. Eur. J.* **2017**, *23*, 12892-12899.

(8) Hamid, A. M; Bera, P. P.; Lee, T. J.; Aziz, S. G.; Alyoubi, A. O.; El-Shall, M. S. Evidence for the Formation of Pyrimidine Cations From The Sequential Reactions of Hydrogen Cyanide with The Acetylene Radical Cation *J. Phys. Chem. Lett.* **2014**, *5*, 3392-3398.

(9) Carvalho, Tânia M.T; Amaral, Luísa M.P.F.; Morais, Victor M.F.; Ribeiro da Silva, Maria D.M.C. Calorimetric and Computational Studies for Three Nitroimidazole Isomers *J. Chem. Thermodyn.* **2017**, *105*, 267–275.

(10) Yu, Z.; Bernstein, E. R. On the Decomposition Mechanisms of New Imidazole-Based Energetic Materials *J. Phys. Chem. A* **2013**, *117*, 1756−1764.

(11) Nair, U.R.; Asthana, S.N.; Subhananda Rao, A.; Gandhe, B.R. Advances in High Energy Materials *Def. Sci. J.* **2010**, *60*, 137-151.

(12) Badgujar, D.M.; Talawar, M.B.; Asthana, S.N.; Mahulikar, P.P. Advances in Science and Technology of Modern Energetic Materials: an Overview. *J. Hazard. Mater.* **2008**, *151*, 289-305.

(13) Bhattacharya, A.; Guo, Y; Bernstein, E. R. Nonadiabatic Reaction of Energetic Molecules *Acc. Chem. Res.* **2010**, *43*, 1476-1485.

(14) Yu, Z.; Bernstein E. R. Experimental and Theoretical Studies of the Decomposition of New Imidazole Based Energetic Materials: Model Systems *J. Chem. Phys*. **2012**, *137*, 114303 (pp 11).

(15) Itälä, E.; Tanzer, K.; Granroth, S.; Kooser, K.; Denifl, S.; Kukk, E. Fragmentation Patterns of 4(5)-nitroimidazole and 1-methyl-5-nitroimidazole - The effect of the Methylation. *J. Mass Spectrom.* **2017**, *52*, 770-776.

(16) Steevens, J. A.; Duke, B. M.; Lotufo, G. R.; Bridges, T. S. Toxicity of the Explosives 2,4,6-Trinitrotoluene, Hexahydro-1,3,5-trinitro-1,3,5-triazine, and Octahydro-1,3,5,7-tetranitro-1,3,5,7-tetrazocine in Sediments to Chironomus Ttentans and Hyalella Azteca: Low-Dose Hormesis and High-Dose Mortality *Environ. Toxicol. Chem.* **2002**, *21*, 1475-1482.

(17) Mäkinen, M.; Nousiainen, M.; Sillanpää, M. Ion Spectrometric Detection Technologies for Ultra-traces of Explosives: A Review *Mass Spectrom. Rev* **2011**, *30*, 940-973.

(18) NIST Chemistry WebBook, NIST Standard Reference Database Number 69, edited by P. J. Linstrom and W. G. Mallard (National Institute of Standards Technology, Gaithersburg, MD, 2015), http://webbook.nist.gov (accessed September 01, 2017).

(19) Luijten, W.C.M.M.; van Thuijl, J. Mass Spectrometry of Nitroazoles *Org. Mass Spetrom.* **1981**, *16*, 199-208.

(20) Blyth, R. R.; Delaunay, R.; Zitnik, M.; Krempasky, J.; Slezak, J.; Prince, K. C.; Richter, R.; Vondracek, M.; Camilloni, R.; Avaldi, L. *et al.* The High Resolution Gas Phase Photoemission Beamline, Elettra *J. Electron Spectrosc. Relat. Phenom.* **1999**, *101–103*, 959–964.

(21) Derossi, A.; Lama, F.; Piacentini, M.; Prosperi, T.; Zema, N. High flux and High Resolution Beamline for Elliptically Polarized Radiation in the Vacuum Ultraviolet and Soft X-ray Regions *Rev. Sci. Instrum*. **1995**, *66*, 1718.

(22) Jimenez, P.; Laynez, J.; Claramunt, R.M.; Sanz, D.; Fayet, J.P.; Vertut, M.C.; Catalan, J.; de Paz, J.L.G.; Pfister-Guillouzo, G.; Guimon, C. et al The Problem of the Tautomerism of 4(5)-nitroimidazole: a Theoretical and Experimental Study *New J. Chem.***1989**, *13*, 151-156.

(23) Feketeova´, L.; Plekan, O.; Goonewardane, M.; Ahmed, M.; Albright, A. L.; White, J.; O'Hair, R. A. J.; Horsman, M.R.; Wang, F.; Prince, K. C. Photoelectron Spectra and Electronic Structures of the Radiosensitizer Nimorazole and Related Compounds *J. Phys. Chem. A* **2015**, *119*, 9986–9995.

(24) Plekan, O.; Coreno, M.; Feyer, V.; Moise, A.; Richter, R.; De Simone, M.; Sankari, R.; Prince, K. C. Electronic State Resolved PEPICO Spectroscopy of Pyrimidine *Phys. Scr.* **2008**, *78*, 058105.

(25) Bolognesi, P.; Kettunen, J. A.; Cartoni, A.; Richter, R.; Tosic, S.; Maclot, S.; Rousseau, P.; Delaunay, R.; Avaldi, L. Site- and State-Selected Photofragmentation of 2Br-Pyrimidine *Phys. Chem. Chem. Phys.* **2015**, *17*, 24063–24069.

(26) Satta, M.; Bolognesi, P.; Cartoni, A.; Casavola, A.R.; Catone, D.; Markus, P.; Avaldi, L. Theoretical and Experimental study on Diiodomethane: Ions and Neutrals in the Gas Phase *J. Chem. Phys.* **2015**, *143*, 244312 (pp 8).

(27) Cartoni, A.; Casavola, A. R.; Bolognesi, P.; Borocci, S.; Avaldi, L. VUV Photofragmentation of CH_2I_2: The $[CH_2I–I]^{\bullet+}$ Iso-diiodomethane Intermediate in the I-Loss Channel from $[CH_2I_2]^{\bullet+}$ *J. Phys Chem. A* **2015**, *119*, 3704-3709.

(28) Castrovilli, M.C.; Bolognesi, P.; Cartoni, A.; Catone, D.; O'Keeffe, P.; Casavola, A.R.; Turchini, S.; Zema, N.; Avaldi, L. Photofragmentation of Halogenated Pyrimidine Molecules in the VUV Range *J. Am. Soc. Mass Spectrom.* **2014**, *25*, 351-367.

(29) Marr, G. V.; West, J. B. Absolute Photoionization Cross-Section Tables for Helium, Neon, Argon and Krypton in the VUV Spectral Regions. *At. Data Nucl. Data Tables* **1976**, *18*, 497-508.

(30) Wong, M. W. Vibrational Frequency Prediction using Density Functional Theory *Chem. Phys. Lett.* **1996**, *256*, 391–399.

(31) Gonzalez; C.; Schlegel, H. B. An Improved Algorithm for Reaction Path Following *J. Chem. Phys.* **1989**, *90*, 2154–2161.

(32) Gonzalez, C.; Schlegel, H. B. Reaction Path Following in Mass-Weighted Internal Coordinates *J. Phys. Chem.* **1990**, *94*, 5523–5527.

(33) Ortiz, J. V. Electron Binding Energies of Anionic Alkali Metal Atoms from Partial Fourth Order Electron Propagator Theory Calculations *J. Chem. Phys.* **1988**, *89*, 6348−6352.

(34) von Niessen, W.; Schirmer, J.; Cederbaum, L. S. Computational Methods for the One-Particle Green's Function *Comput. Phys. Rep.* **1984**, *1*, 57−125.

(35) Frisch, M.J.; Trucks, G.W.; Schlegel, H.B.; Scuseria, G.E.; Robb, M.A.; Cheeseman, J.R. Scalmani, G.; Barone, V.; Mennucci, B; Petersson, G. A. *et al.*, Gaussian 09, Revision A.02, Gaussian, Inc., Wallingford, CT, **2009**

(36) He, Y.-L.; Wang, L. Cations of Halogenated Methanes Adiabatic Ionization Energies, Potential Energy Surfaces, and Ion Fragment Appearance Energies *Struct. Chem.* **2009**, *20*, 461-479.

(37) Schwell, M.; Jochims, H.-W.; Baumgärtel, H.; Leach, S. VUV Photophysics and Dissociative Photoionization of Pyrimidine, Purine, Imidazole and Benzimidazole in the 7-18 eV photon energy range *Chem. Phys.* **2008**, *353*, 145-162.

(38) Klebe, K.J.; Houte, J.J.V.; Thuijl, J.V. Loss of HCN and H from the molecular ion of imidazole *Org. Mass Spectrom.*, **1972**, 6, 1363-1368

(39) Kokkila Schumacher, S. I. L.; Bera, P. P.; Lee, T. J. Characterization of the Azirinyl Cation and Its Isomers *J. Phys. Chem. A* **2016**, *120*, 1275−1282.

(40) Talbi, D. An Extensive Ab Initio Study of a Process of Astrophysical Interest: The $N^+(N)+CH_3(CH_3^+)$ Reaction *Chem. Phys. Lett.* **1999**, *312*, 291-298.

(41) McLafferty, F.W.; McCilvery, D. C. Collisional Activation and Metastable Ion Characteristics. 79. Gaseous HCN^+, HNC^+, and $HCNH^+$ ions *J. Am. Chem. Soc.* **1980**, *102*, 6189-6190.

(42) Brites, V.; Jutier, L. New Ab initio Study of The Spectroscopy of $HCNH^+$ *J. Mol. Spectrosc.* **2012**, *271*, 25-32.

(43) Demarais, N. J.; Yang, Z.; Snow, T.P.; Bierbaum, V.M. Chemistry of $HCNH^+$: Mechanisms, Structures, and Relevance to Titan's Atmosphere *Struct. Chem.* **2013**, *24*, 1957-1963.

(44) Jung, S.H.; Choe, J.C. Mechanisms of Prebiotic Adenine Synthesis from HCN by Oligomerization in The Gas Phase *Astrobiology* **2013**, *13*, 465-475

(45) McLain, J.L.; Adams, N.G. Flowing Afterglow Studies of Temperature Dependencies for Electron Dissociative Recombination of $HCNH^+$, CH_3CNH^+ and $CH_3CH_2CNH^+$ and Their Symmetrical Proton-Bound Dimers *Planet. Space Sci* **2009**, *57*,1642-1647.

(46) Ziurys, L. M.; Turner, B. E. HCNH ($^+$)-A New Interstellar Molecular Ion *Astrophys. J.* **1986**, *302*: L31-L36

(47) Milligan, D. B.; Freeman, C. G.; Maclagan, R. G. A. R.; McEwan, M. J.; Wilson, P.F.; Anicich, V.G. Termolecular ion–molecule reactions in Titan's atmosphere. II: the structure of the association adducts of $HCNH^+$ with C_2H_2 and C_2H_4 *J. Am. Soc. Mass Spectrom.* **2001**, *12*, 557–564

(48) Lau, K-C; Li, W-K; Chiu, S.-W. A Gaussian-2 Study of Isomeric C_2H_2N and $C_2H_2N^+$ *J. Phys. Chem. A* **1999**, *103*, 3330−3335.

(49) Harland, P.W.; Maclagan, R.G.A.R.; Schaefer, H.F. Structures and Energies of $C_2NH^+_2$ Isomers *J. Chem. Soc. Faraday Trans. 2*, **1989**, *85*, 187-193

(50) Frankowski, M.; Sun, Z., Smith-Gicklhorn, A. M. Unraveling The Possible Isomers of CH_4 CN^+ and CH_2CN^+ Through FT-IR Matrix-Isolation Spectroscopy of Mass-Selected Ions and DFT Theory *Phys. Chem. Chem. Phys.* **2005**, *7*, 797-805.

(51) Cartoni, A.; Catone, D.; Bolognesi, P.; Satta, M.; Markus, P.; Avaldi, L. HSO_2^+ Formation from Ion-Molecule Reactions of $SO_2^{\cdot+}$ with Water and Methane: Two Fast Reactions with Reverse Temperature-Dependent Kinetic Trend *Chem. Eur. J.* **2017**, *23*, 6772–6780.

(52) Dujardin, G.; Leach, S. Photoion–Fluorescence Photon Coincidence Study of Radiative and Dissociative Relaxation Processes in VUV Photoexcited SO_2. Fluorescence of SO^+_2, SO^+, and SO *J. Chem. Phys.* **1981**, *75*, 2521 –2531.

(53) Lévêque, C.; Köppel, H.; Taïeb, R. Excited State Dynamics in SO_2. III. An Ab Initio Quantum Study of Single- and Multi-Photon Ionization *J. Chem. Phys.* **2014**, *140*, 204303 (pp 11).

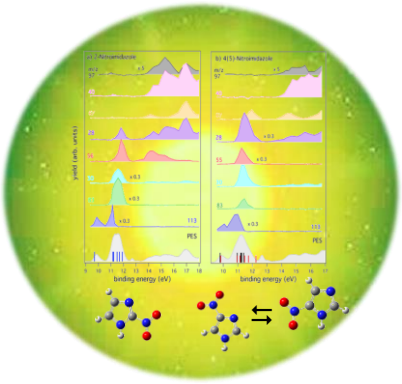

TOC Graphic